Multi-channel analysis of surface waves (MASW) of models with high shear-wave velocity contrast

Julian Ivanov,* Richard D. Miller, Shelby Peterie, Chong Zeng, Jianghai Xia, and Tyler Schwenk
Kansas Geological Survey, The University of Kansas

Summary

We use the multi-channel analysis of surface waves (MASW) method to analyze synthetic seismic data calculated using models with high shear-wave velocity (V_s) contrast. The MASW dispersion-curve images of the Rayleigh wave are obtained using various sets of source-offset and spread-size configurations from the synthetic seismic data and compared with the theoretically calculated fundamental- and higher-mode dispersion-curves. Such tests showed that most of the dispersion-curve images are dominated by higher-mode energy at the low frequencies, especially when analyzing data from long receiver offsets and thus significantly divert from numerically expected dispersion-curve trends, which can lead to significant V_s overestimation. Further analysis showed that using data with relatively short spread lengths and source offsets can image the desired fundamental-mode of the Rayleigh wave that matches the numerically expected dispersion-curve pattern. As a result, it was concluded that it might be possible to avoid higher-mode contamination at low frequencies at sites with high (V_s) contrast by appropriate selection of spread size and seismic source offset.

Introduction

Stiffness properties of near-surface materials are important for various environmental and engineering applications. Stiffness is directly related to shear-wave velocity (V_s), V_s increases as material shear strength (stiffness, rigidity) increases. V_s can be estimated by analyzing surface waves on seismic data. We use the multichannel analysis of surface waves (MASW) method to estimate near-surface shear-wave velocity from high-frequency (≥ 2 Hz) Rayleigh-wave data (Miller et al., 1999a; Song et al., 1989; Park et al., 1998; Xia et al., 1999a). Shear-wave velocities estimated using MASW have reliably and consistently correlated with drill data. Using the MASW method, Xia et al. (2000) noninvasively measured V_s within 15% of V_s measured in wells. Miller et al. (1999a) mapped bedrock with 0.3-m (1-ft) accuracy at depths of about 4.5-9 m (15-30 ft), as confirmed by numerous borings. The MASW method has been applied to problems such as characterization of pavements (Ryden et al., 2004), the study of Poisson's ratio (Ivanov et al., 2000), study of levees and subgrade (Ivanov et al., 2005; Ivanov et al., 2006b), investigation of sea-bottom sediment stiffness (Ivanov et al., 2000; Kaufman et al., 2005; Park et al., 2005a), mapping of fault zones (Ivanov et al., 2006c), study of Arctic ice sheets (Ivanov et al., 2009, Tsoflias et al., 2008), detection of dissolution features (Miller et al., 1999b), and measurement of S-wave velocity as a function of depth (Xia et al., 1999b). Studies of the MASW method have been extended to areas of determination of near-surface Q (Xia et al., 2002), and the acquisition of more realistic seismic refraction models (Ivanov et al., 2006a; Ivanov et al., 2010).

The MASW method is applied by performing the following steps. A single seismic-data record is acquired by a set of low-frequency (e.g., 4.5 Hz) geophones evenly spaced along a line. The seismic data from such a shot record is transformed into a phase-velocity – frequency domain image (i.e., dispersion-curve image), which is used to evaluate the dispersion-curve trend of the fundamental-mode of the Rayleigh wave. The estimated dispersion curve is then inverted to produce a 1-D Vs model (Xia et al., 1999a), which is assigned to the middle of the geophone spread. By assembling numerous 1-D Vs models derived from consecutively recorded seismic shot records along a seismic line, a 2-D V_s model can be obtained.

Most recent developments of the MASW method include the expansion of the traditional fundamental-mode dispersion-curve inversion with the inclusion and inversion of higher modes (Xia et al., 2003; Beaty et al., 2002; Beaty and Schmitt, 2003; Luo et al., 2007). It was reported that the addition of first and second higher-mode dispersion curves reduced the relative error of inversion results (compared to borehole data) to 3.6% in comparison to 15% when only the fundamental-mode dispersion-curve data was used for the inversion process.

However, the imaging and quality of the fundamental- and higher-modes dispersion-curve trends, essential for the method, can be influenced by field data acquisition parameters such as geophone spread length and source offset. Optimum minimum-receiver offset and spread-length determinations extending from the spectral analysis of surface waves (SASW) method, which uses as few as 2 geophones (Heisey et al., 1982; Roesset et al., 1989), have been the subject of further research when using the MASW method (Park et al., 2001; Zhang et al., 2004; Xu et al., 2006). As a result of that research, recommendations and rules of thumb were developed that could easily be implemented in practice. These efforts were extended by Ivanov et al. (2008) who recommended the acquisition of a series of dispersion-curve images using various combinations of source-offset and spread-size parameters to select the set that provides the optimal dispersion-curve images. Sets with non-optimal parameters typically produced images with higher-mode domination for

most of the higher frequencies. However, some researchers have reported that at some sites higher-mode energy can dominate over the fundamental mode at the low-frequency end of the spectrum (Park et al., 2005b, Ivanov et al., 2009). Such higher-mode domination was demonstrated using models with high shear-wave velocity contrasts (Levshin and Panza, 2006; Cercato et al., 2010). One of the models suggested by Levshin and Panza (2006) consisted of two layers (Table 1) and had high contrast for both shear (V_s) and compressional (V_p) wave velocities.

Layer	V_s(m/s)	V_p(m/s)	Dens. (g/m^3)	Thick (m)
1	500	1000	1.8	10
2	1500	3000	1.8	∞

Table 1. The two-layer model parameters used for the calculation of synthetic seismic data.

The 2-layer model parameters were used by two different modeling algorithms. One (Zeng et al., 2011) calculated a synthetic seismic record (Figure 1).
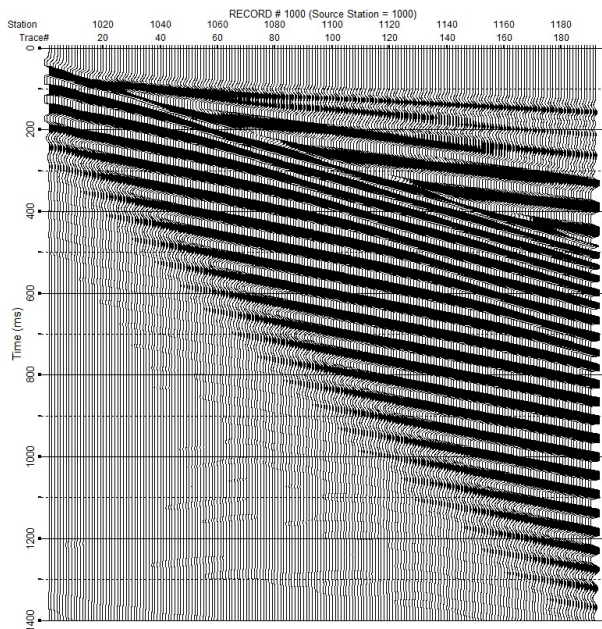

Figure 1. Synthetic seismic data estimated using the velocity model in Table 1.

Another algorithm (Schwab and Knopoff, 1972) was used to calculate the theoretical dispersion curves of the fundamental and the first higher modes. The synthetic seismic record was used to generate a corresponding dispersion-curve image (Park et al., 1998), on which the calculated dispersion curves were plotted on top for comparison (Figure 2).
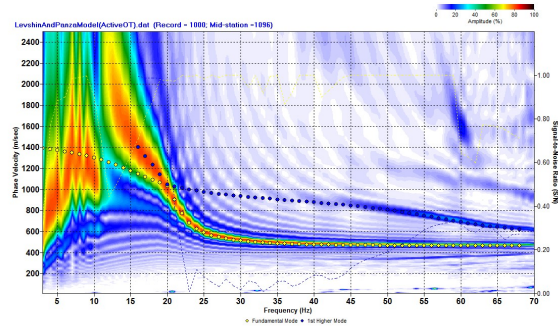

Figure 2. Dispersion-curve image of the synthetic seismic record and the estimated fundamental (yellow dots) and first higher (dark dots) modes.

These results (Figure 2) were very similar to Cercato et al. (2010). They illustrate that when dealing with such high velocity contrast models the dispersion-curve image is dominated by higher-mode energy below a certain frequency (i.e., 20 Hz on Figure 2) instead of the fundamental-mode. As a result, the V_s and corresponding rigidity can be significantly overestimated, which can potentially lead to detrimental consequences for certain projects (e.g., engineering, environmental, etc.) using this type of data.

Such higher-mode domination at the low-frequency end is very atypical because for most earth models it usually occurs (e.g., Ivanov et al., 2008) at the higher-frequency portion of the dispersion-curve images (i.e., higher-mode frequency ranges are relatively shifted toward the higher frequencies).

Following the example of Ivanov et al. (2008), we investigated if such higher-mode interference over fundamental-mode imaging at the low frequencies (i.e., below 20 Hz) can be resolved (or reduced) by using a specific combination of spread-size and source-offset parameters. After producing a series of dispersion-curve images using various combinations of source-offset and spread-size parameters, it was possible to find sets that provided dispersion-curve image trends that follow the theoretically calculated fundamental-mode dispersion curve.

Results

The synthetic seismic data for the 2-layer model (Table 1) was calculated for a record with 192 channels spaced every 1 m, the source 1 m away from the first geophone, and a 20 Hz Ricker wavelet (Figure 1). Various ways of higher-mode interference over the fundamental-mode below 20 Hz can be observed on the phase-velocity – frequency domain images produced by applying the dispersion-curve transform to portions of synthetic seismic data with source offsets at 1, 20, 40, and 60 and spreads of 95 m (Figure 3) and 30 m (Figure 4).
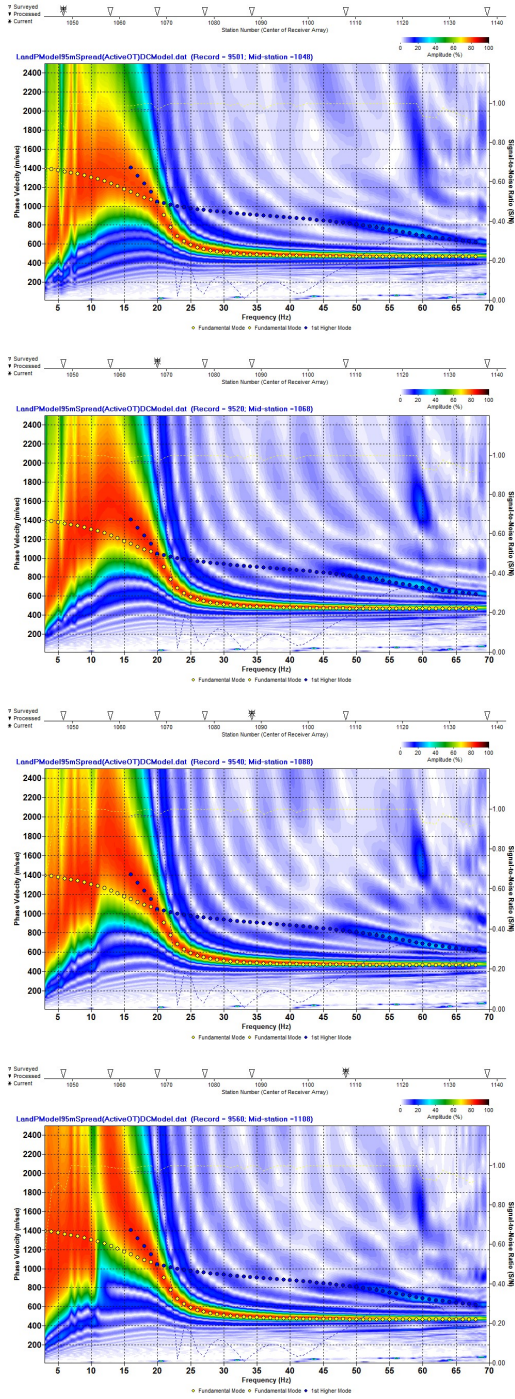
MASW and high Vs contrast

Figure 3. Dispersion-curve images of a 95-m wide spread synthetic data and source offset at 1 m (a), 20 m (b), 40 m (c), and 60 m (d) with calculated fundamental (yellow dots) and first higher (dark dots) modes. a) to d) are from top to bottom.
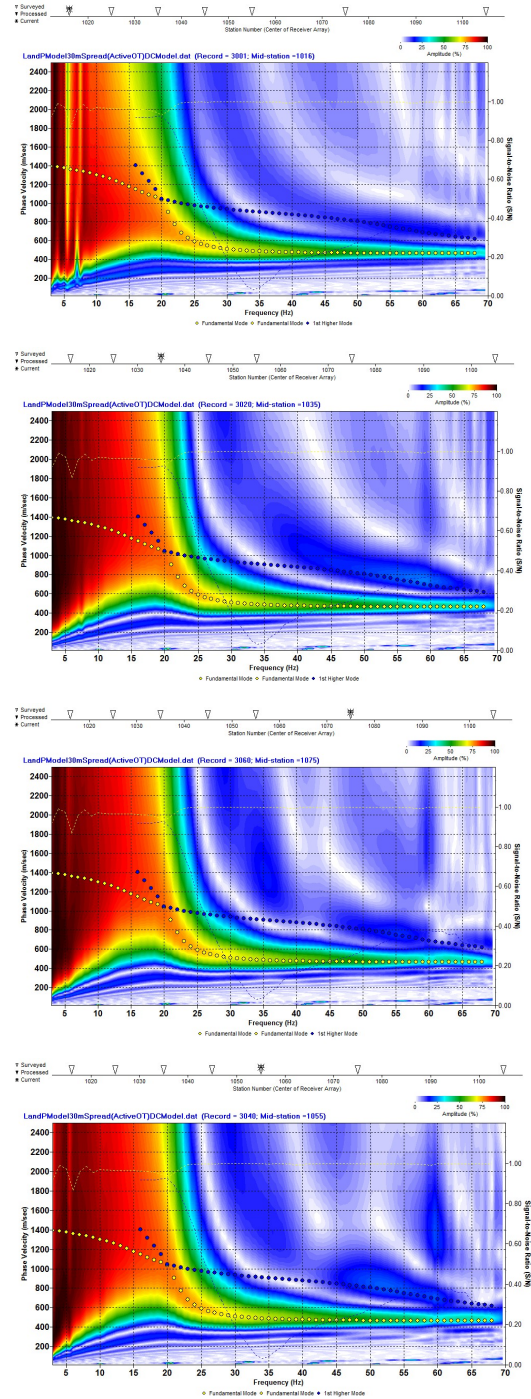
Figure 4. Dispersion-curve images of a 30-m wide spread synthetic data and source offset at 1 m (a), 20 m (b), 40 m (c), and 60 m d) with calculated fundamental (yellow dots) and first higher (dark dots) modes. . a) to d) are from top to bottom.

Using all available channels (192) and thus the longest spread (191 m) the dispersion-curve image with best contrast possible was obtained (Figure 2), which is consistent with existing research (Xu et al., 2006). However, the trend with maximum energy clearly follows the direction of the first higher mode from about 20 to 12 Hz instead of the fundamental mode.

Using half the channels, a 95-m spread with a 90 m source offset (and thus ignoring the first 96 channels of the original synthetic record) a similar dispersion-curve image was produced with somewhat poorer contrast (Figure 5a). Moving the spread closer to the source from 60 to 1 m resulted in images (Figure 3), with dominant dispersion-curve trends between 20 and 10 Hz that gradually shift toward the calculated fundamental-mode (yellow dots) dispersion curve, but never reached it. Such inaccuracy could result in various degrees of overestimation of the fundamental-mode, if these sets of spread size and source offset were used.
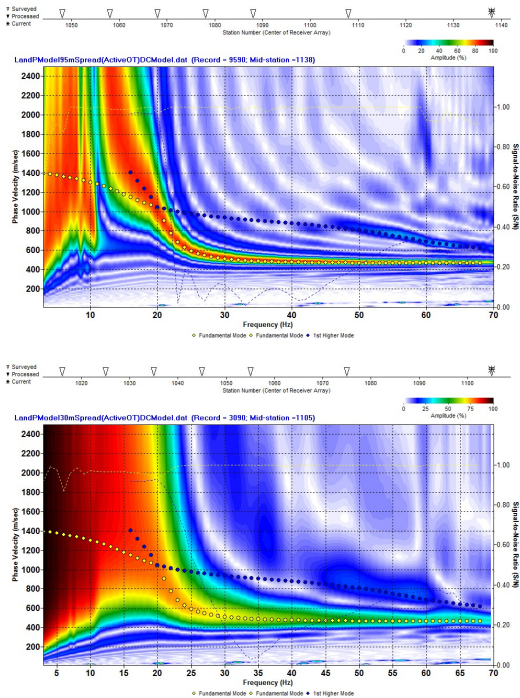

Figure 5. Dispersion-curve images of the synthetic seismic record using 90 m source offset and 95 m a), and 30 m b) spread with the theoretically calculated fundamental (yellow dots) and first higher (dark dots) modes.

Using the same set of source offsets with a significantly shorter spread of 30 m resulted in obtaining dispersion-curve images with significantly blurrier contrast below 20 Hz (Figure 4), where dispersion-curve energy was spread more

than 3 times wider in comparison to the images from the 90-m spreads. However, in spite of the blurriness, the maximum peak of the dispersion-curve energy below 20 Hz matches almost perfectly with the dispersion-curve trend of the calculated fundamental-mode using source offset at 20 to 40 m from the spread. As the source offset increased to 60 m (Figure 4d) and 90 m (Figure 5b), the higher-mode energy influenced the maximum ridge of the blurred dispersion-curve energy below 20 Hz more.

It is difficult to estimate fundamental-mode energy with 90 m source-offset data (Figure 5) regardless of whether the spread length is short (30 m) or long (90 m), which illustrates the higher-mode domination at far offsets at low frequencies.

Conclusions

This work confirmed that when there is a high-velocity contrast 2-layer model, the low-frequency range of the dispersion-curve images might be strongly influenced and dominated by higher-mode energy.

Our analysis demonstrates that such higher-mode domination at low frequencies can be minimized or reduced by optimal selection of receiver-offset and spread-size parameters, which we consider to be the main contribution of this research. Currently, we think that from a practical perspective such a data set selection is most reliably performed through a series of tests, as was demonstrated in this manuscript.

Still, the suggested approach may come at the price of low resolution at low frequencies (i.e., below 20 Hz), which can make dispersion-curve picking at that range challenging.

The observation that higher modes become stronger at longer offset, in general, is consistent with previous research. However, the conventional expectation is that to should be observed at relatively higher frequencies. This work emphasizes the possibility for that to happen at the low-frequency end of the dispersion-curve spectrum.

This research shows that it is possible to make correct identification and estimation of the fundamental-mode of the Rayleigh wave dispersion-curve data even when dealing with high-velocity contrast models. Thus, the inversion can produce accurate V_s results and V_s overestimation at greater depths due to higher-modes interference can be avoided.

EDITED REFERENCES

Note: This reference list is a copy-edited version of the reference list submitted by the author. Reference lists for the 2011 SEG Technical Program Expanded Abstracts have been copy edited so that references provided with the online metadata for each paper will achieve a high degree of linking to cited sources that appear on the Web.

REFERENCES

Beaty, K. S., and D. R. Schmitt, 2003, Repeatability of multimode Rayleigh-wave dispersion studies: Geophysics, **68**, 782–790, doi:10.1190/1.1581031.

Beaty, K. S., D. R. Schmitt, and M. Sacchi, 2002, Simulated annealing inversion of multimode Rayleigh wave dispersion curves for geological structure: Geophysical Journal International, **151**, no. 2, 622–631, doi:10.1046/j.1365-246X.2002.01809.x.

Cercato, M., F. Cara, E. Cardarelli, G. Di Filippo, G. Di Guilio, and G. Milana, 2010, Surface-wave velocity profiling at sites with high stiffness contrast: A comparison between invasive and noninvasive methods: Near Surface Geophysics, **8**, 75–94.

Heisey, J. S., K. H. Stokoe II, W. R. Hudson, and A. H. Meyer, 1982, Determination of in situ shear-wave velocity from spectral analysis of surface waves: Research Report No. 256-2, Center for Transportation Research, The University of Texas at Austin.

Ivanov, J., R. D. Miller, J. B. Dunbar, and S. Smullen, 2005, Time-lapse seismic study of levees in southern Texas: 75th Annual International Meeting, SEG, Expanded Abstracts, 1121–1124.

Ivanov, J., R. D. Miller, P. J. Lacombe, C. D. Johnson, and J. W. Lane Jr., 2006a, Delineating a shallow fault zone and dipping bedrock strata using multichannel analysis of surface waves with a land streamer: Geophysics, **71**, no. 5, A39–A42. doi:10.1190/1.2227521

Ivanov, J., R. D. Miller, P. J. Lacombe, C. D. Johnson, and J. W. Lane Jr., 2006b, Delineating a shallow fault zone and dipping bedrock strata using multichannel analysis of surface waves with a land streamer: Geophysics, **71**, no. 5, A39–A42. doi:10.1190/1.2227521

Ivanov, J., R. D. Miller, N. Stimac, R. F. Ballard, J. B. Dunbar, and S. Smullen, 2006c, Time-lapse seismic study of levees in southern Texas: 76th Annual International Meeting, SEG, Expanded Abstracts, 3255–3258.

Ivanov, J., R. D. Miller, and G. Tsoflias, 2008, Some practical aspects of MASW analysis and processing: SAGEEP, no. 1, 1186–1198.

———, 2009, Practical aspects of MASW inversion using varying density: SAGEEP, 171–177.

Ivanov, J., R. D. Miller, J. Xia, J. B. Dunbar, and S. L. Peterie, 2010, Refraction nonuniqueness studies at levee sites using the refraction-tomography and JARS methods, *in* R. D. Miller, J. D. Bradford, and K. Holliger, eds., Advances in near-surface seismology and ground-penetrating radar: SEG Geophysical Developments Series No. 15, 327–338.

Ivanov, J., R. D. Miller, J. Xia, D. Steeples, and C. B. Park, 2006d, Joint analysis of refractions with surface waves — An inverse solution to the refraction-travel-time problem: Geophysics, **71**, no. 6, R131–R138, doi:10.1190/1.2360226.

Ivanov, J., S. Peterie, C. D. Johnson, J. W. Lane, R. D. Miller, and D. Clemens, 2009, Near-surface evaluation of Ball Mountain Dam, Vermont, using multichannel analysis of surface waves (MASW) and refraction tomography seismic methods on land-streamer data: 79th Annual International Meeting, SEG, Expanded Abstracts, 28, no. 1, 1454–1458.

Ivanov, J. M., C. B. Park, R. D. Miller, and J. Xia, 2000, Mapping Poisson's ratio of unconsolidated materials from a joint analysis of surface-wave and refraction events: SAGEEP.

Kaufmann, R. D., J. Xia, R. Benson, L. B. Yuhr, D. W. Casto, and C. B. Park, 2005, Evaluation of MASW data acquired with a hydrophone streamer in a shallow marine environment: Journal of Environmental & Engineering Geophysics, **10**, no. 2, 87–98, doi:10.2113/JEEG10.2.87.

Levshin, A. L., and G. F. Panza, 2006, Caveats in multimodal inversion of seismic surface wavefields: Pure and Applied Geophysics, **163**, no. 7, 1215–1233, doi:10.1007/s00024-006-0069-3.

Luo, Y., J. Xia, J. Liu, Q. Liu, and S. Xu, 2007, Joint inversion of high-frequency surface waves with fundamental and higher modes: Journal of Applied Geophysics, **62**, no. 4, 375–384, doi:10.1016/j.jappgeo.2007.02.004.

Miller, R. D., J. Xia, C. B. Park, J. Davis, W. Shefchik, and L. Moore, 1999b, Seismic techniques to delineate dissolution features in the upper 1000 ft at a power plant: 69th Annual International Meeting, SEG, Expanded Abstracts, 492–495.

Miller, R. D., J. Xia, C. B. Park, and J. M. Ivanov, 1999a, Multichannel analysis of surface waves to map bedrock: The Leading Edge, **18**, 1392–1396, doi:10.1190/1.1438226.

Park, C. B., R. D. Miller, N. Ryden, J. Xia, and J. Ivanov, 2005a, Combined use of active and passive surface waves: Journal of Environmental & Engineering Geophysics, **10**, no. 3, 323–334, doi:10.2113/JEEG10.3.323.

Park, C. B., R. D. Miller, and J. Xia, 1998, Imaging dispersion curves of surface waves on multi-channel record: 68th Annual International Meeting, SEG, Expanded Abstracts, 1377–1380.

———, 2001, Offset and resolution of dispersion curve in multichannel analysis of surface waves (MASW): SAGEEP.

Park, C. B., R. D. Miller, J. Xia, J. Ivanov, G. V. Sonnichsen, J. A. Hunter, R. L. Good, R. A. Burns, and H. Christian, 2005b, Underwater MASW to evaluate stiffness of water-bottom sediments: The Leading Edge, **24**, 724–728, doi:10.1190/1.1993267.

Roesset, J. M., D. W. Chang, K. H. Stokoe II, and M. Aouad, 1989, Modulus and thickness of the pavement surface layer from SASW tests: Transportation Research Record, no. 1260, 53–63.

Ryden, N., C. B. Park, P. Ulriksen, and R. D. Miller, 2004, Multimodal approach to seismic pavement testing: Journal of Geotechnical and Geoenvironmental Engineering, **130**, no. 6, 636–645, doi:10.1061/(ASCE)1090-0241(2004)130:6(636).

Song, Y. Y., J. P. Castagna, R. A. Black, and R. W. Knapp, 1989, Sensitivity of near-surface shear-wave velocity determination from Rayleigh and Love waves: 59th Annual International Meeting, SEG, Expanded Abstracts, 509–512.

Schwab, F. A., and L. Knopoff, 1972, Fast-surface wave and free mode computations; in Methods in Computational Physics: Academic Press.

Tsoflias, G.P., J. Ivanov, S. Anandakrishnan, H. Horgan, L. Peters, D. Voigt, and P. Winberry, 2008, Firm and shallow ice profiling at Jakobshavn Glacier using dispersed seismic surface waves: EOS Transactions, AGU.

Xia, J., R. D. Miller, C. B. Park, and G. Tian, 2002, Determining Q of near-surface materials from Rayleigh waves: Journal of Applied Geophysics, **51**, no. 2–4, 121–129, doi:10.1016/S0926-9851(02)00228-8.

———, 2003, Inversion of high-frequency surface waves with fundamental and higher modes: Journal of Applied Geophysics, **52**, no. 1, 45–57, doi:10.1016/S0926-9851(02)00239-2.

Xia, J., R. D. Miller, and C. B. Park, 1999a, Estimation of near-surface shear-wave velocity by inversion of Rayleigh waves: Geophysics, **64**, 691–700, doi:10.1190/1.1444578.

Xia, J., R. D. Miller, C. B. Park, J. A. Hunter, and J. B. Harris, 1999b, Evaluation of the MASW technique in unconsolidated sediments: 69th Annual International Meeting, SEG, Expanded Abstracts, 437-440.

———, 2000, Comparing shear-wave velocity profiles from MASW with borehole measurements in unconsolidated sediments, Fraser River Delta, B.C., Canada: Journal of Environmental & Engineering Geophysics, **5**, no. 3, 1–13, doi:10.4133/JEEG5.3.1.

Xu, Y., J. Xia, and R. D. Miller, 2006, Quantitative estimation of minimum offset for multichannel surface-wave survey with actively exciting source: Journal of Applied Geophysics, **59**, 117–125, doi:10.1016/j.jappgeo.2005.08.002.

Zeng, C., J. Xia, R. D. Miller, and G. P. Tsoflias, 2011, Application of the multiaxial perfectly matched layer (M-PML) to near-surface seismic modeling with Rayleigh wave: Geophysics, 76, no. 3, T43–T52.

Zhang, S. X., L. S. Chan, and J. Xia, 2004, The selection of field acquisition parameters for dispersion images from multichannel surface wave data: Pure and Applied Geophysics, **161**, no. 185, 1–17, doi:10.1007/s00024-003-2428-7.